JACS
JOURNAL OF THE AMERICAN CHEMICAL SOCIETY
Article
pubs.acs.org/JACS

$Ni_9Te_6(PEt_3)_8C_{60}$ Is a Superatomic Superalkali Superparamagnetic Cluster Assembled Material (S^3-CAM)

Vikas Chauhan, Sanjubala Sahoo, and Shiv N. Khanna*

Department of Physics, Virginia Commonwealth University, Richmond, Virginia 23284-2000, United States

Supporting Information

ABSTRACT: First-principles theoretical studies enable an electronic and magnetic characterization of the recently synthesized $Ni_9Te_6(PEt_3)_8C_{60}$ ionic material consisting of $Ni_9Te_6(PEt_3)_8$ superatoms and C_{60}. The PEt_3 ligands are shown to create an internal coulomb well that lifts the quantum states of the Ni_9Te_6 cluster, lowering its ionization potential to 3.39 eV thus creating a superalkali motif. The metallic core has a spin magnetic moment of 5.3 μ_B in agreement with experiment. The clusters are marked by low magnetic anisotropy energy (MAE) of 2.72 meV and a larger intra-exchange coupling exceeding 0.2 eV, indicating that the observed paramagnetic behavior around 10K is due to superparamagnetic relaxations. The magnetic motifs separated by C_{60} experience a weak superexchange that stabilizes a ferromagnetic ground state as observed around 2 K. The calculated MAE is sensitive to the charged state that could account for the observed change in magnetic transition temperature with size of the ligands or anion.

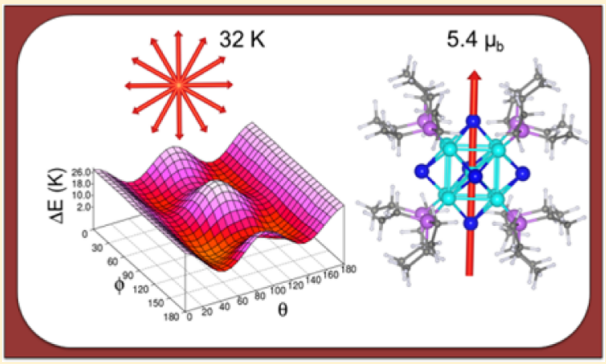

INTRODUCTION

One of the promising directions in cluster science is to synthesize hierarchical solids where atomic clusters serve as elemental building blocks. Such materials are unique in that they combine the intracluster and intercluster length scales and hence offer novel ways to tune the properties of the assembled material.[1−8] However, synthesizing such materials faces various challenges including identifying the superatomic building blocks or composite units that would maintain their identity upon assembly.[9−11] There are also fundamental issues such as formulating a set of principles that direct the formation of the ordered phase and understanding the collective behaviors that emerge as the individual units are collected into the ordered phase. One approach, that has been highly successful, is to use ligated clusters, as the ligands can prevent the coalescence of clusters.[12−15] Over the past decade, numerous such assemblies composed of Au_n, Ag_n, and mixed species ligated with a variety of ligands have been synthesized and characterized.[12,16] These assemblies contain clusters of precise size and composition that can be controlled by varying the experimental conditions, and the resulting materials have shown novel physical and chemical properties that can be tuned with size. The stability of most of these assemblies with metallic cores has been rationalized within a superatomic picture where the ligands undergo covalent bonding with selected electronic states leading to clusters with filled superatomic shells.

Recently, Roy et al. have reported synthesizing cluster solids from an assembly of individually synthesized chalcogenide superatoms that exchange charge with counterions to form ionic solids.[17] One such assembly consists of $Ni_9Te_6(PEt_3)_8$ clusters composed of a Ni_9Te_6 core decorated with eight triethylphosphine (PEt_3) ligands attached to Ni sites. The cluster had previously been isolated as an intermediate species during the synthesis of the bulk NiTe from organometallic reagents serving as sources of Ni and Te.[18] This is, however, the first time that $Ni_9Te_6(PEt_3)_8$ is shown to form a rock-salt (NaCl) structure where the ligated cluster acts as an electron donor when combined with C_{60} as an electron acceptor. More recent experiments indicate that the ionic solid is magnetic and undergoes a ferromagnetic phase transition at low temperatures (4K), while it exhibits Curie−Weiss behavior at higher temperatures (above 10 K).[19] The SQUID measurements also indicate that the individual clusters behave as isolated localized magnets with a magnetic moment of around 5.4 μ_B per functional unit. Additional magnetic measurements on $Ni_9Te_6(PMe_3)_8C_{60}$ with trimethylphosphine ligands and on $Ni_9Te_6(PEt_3)_8C_{70}$ brought out new features. Because of a smaller ligand shell, $Ni_9Te_6(PMe_3)_8C_{60}$ has a smaller superatom-to-superatom separation, and it was found to increase the magnetic transition temperature (T_M) to 7 K. On the other hand, the large size of C_{70} leads to larger lattice parameter than in $Ni_9Te_6(PEt_3)_8C_{60}$ and was shown to reduce the T_M to around 2.5 K. These observations raise several fundamental issues. The chalcogenide cluster Ni_9Te_6 has a high ionization potential of 5.88 eV (as we will show in this study). The PEt_3 ligands also have a high ionization potential of 7.98 eV. How does then the addition of PEt_3 ligands change the

Received: October 20, 2015
Published: January 20, 2016

DOI: 10.1021/jacs.5b10986
J. Am. Chem. Soc. 2016, 138, 1916−1921

electronic feature of cluster to make it an electron donor? This is critical to the formation of the ionic assembly as C_{60}, with an electron affinity (EA) of 2.68 eV that acts as an electron acceptor. This could also shed light on the role of ligands in promoting the formation of the ionic solid. On the magnetic side, an estimation of the exchange coupling within each individual cluster would clarify if the solid undergoes a paramagnetic or superparamagnetic relaxations above 10 K. In addition, the characterization of magnetic anisotropies of these solids is needed to understand the nature of the magnetic transition at low temperatures. The ferromagnetic phase and the hysteresis at 2 K require magnetic coupling between the superatoms. What is the origin of this coupling and are the MAE and coupling sensitive to the charge state of the clusters? These could provide an understanding of the change in T_M as one modulates the superatom−superatom separation that could change the charged state of the clusters.

In this work we have carried out first-principles electronic structure calculations to offer insight into the above electronic and magnetic issues. The role of ligands in protecting the clusters is well-known, but their role in promoting formation of assemblies has not been widely highlighted. As we will show, the ligands are critical to the formation of the ionic solid. We also investigate the exchange coupling between the spins within the $Ni_9Te_6(PEt_3)_8$ cluster and show that it is much higher than the MAE. Consequently, the solid undergoes a ferromagnetic−superparamagnetic transition above 4 K. Experiments indicate that the T_M is sensitive to the nature of the ligand. To make contact with these experiments, we also analyze the effect of ligands on the MAE and show that the spin hypersurface and the MAE are sensitive to the charged state of the cluster.

METHODS

The electronic structure calculations are performed using Vienna ab initio simulation package (VASP) in the framework of density functional theory (DFT). The generalized gradient approximation (GGA) for exchange−correlation potential as proposed by Perdew−Burke−Ernzerhof (PBE) is taken.[20] The Kohn−Sham equations are solved using periodic boundary conditions with the plane-wave basis set. The projector-augmented wave method is used to represent the electron−ion interaction.[21] The energy cutoff for the plane-wave basis is set to 500 eV. The cluster calculations are performed using only one *k*-point, i.e., at the Γ-point. The $Ni_9Te_6(PEt_3)_8$ and Ni_9Te_6 clusters are kept in supercell of size 25 × 25 × 25 Å^3 and 18 × 18 × 18 Å^3, respectively; large enough to minimize the interactions between the cluster and its periodic images. The structural optimization is done using the conjugate gradient method.[22,23] The tolerance for the total energy change during structural optimization was set to 10^{-6} eV. The local moment is calculated by the integration of the spin densities over atom-centered spheres as implemented in VASP. In order to calculate the MAE, we performed non-self-consistent calculations with the SOI (implemented in VASP by Kresse and Lebacq),[24] where the charge density is kept fixed as obtained from the self-consistent scalar-relativistic calculation. Furthermore, some calculations for the neutral and charged species with several spin multiplicities are performed using another DFT-based code, namely, ADF within GGA-PBE for the exchange and correlation functional. The atomic wave functions are expressed in terms of Slater-type orbitals. A TZ2P basis set and a large frozen electron core were used.[25] Scalar relativistic effects were incorporated using the zero-order regular approximation (ZORA).[26,27]

RESULTS AND DISCUSSIONS

Our investigations started with electronic structure of bare and ligated Ni_9Te_6 clusters using the VASP with supercell approach.[28,29] Supplementary calculations have also been carried out using the Amsterdam Density Functional (ADF) code to study free clusters using localized basis.[30,31] Unless specifically mentioned, we present results based on the VASP. The $Ni_9Te_6(PEt_3)_8$ building block is composed of a body-centered cube of Ni sites with faces decorated by six Te atoms, while eight PEt_3 ligands are attached to the Ni sites. Figure 1

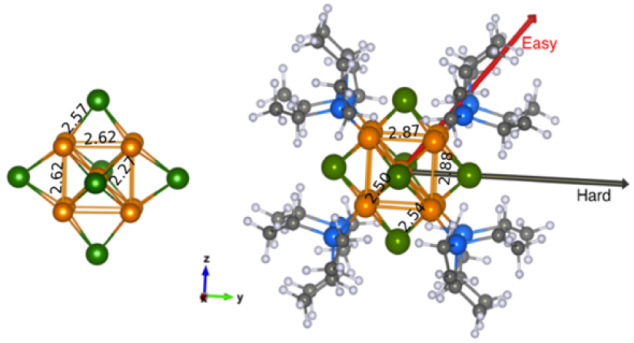

Figure 1. Ground-state structures (a) Ni_9Te_6 and (b) $Ni_9Te_6(PEt_3)_8$. The Ni, Te, P, C, O, and H atoms are shown in gold, green, blue, gray, and white colors, respectively. The easy axis (red arrow) corresponds to ϕ = 135° and θ = 50°, while the hard axis (black arrow) corresponds to ϕ = 90° and θ = 90°. The average bond lengths are given in Å (see Figure 4 for the definition of ϕ and θ).

shows the optimized ground-state structure of the bare and ligated Ni_9Te_6 cluster. Ni_9Te_6 has a ground state with a spin moment of 6 μ_B. The average Ni−Ni and Ni−Te distances are 2.62 and 2.57 Å, respectively. The addition of ligands does not influence the spin state of Ni_9Te_6, i.e., $Ni_9Te_6(PEt_3)_8$ has the same multiplicity. The average Ni−Ni and Ni−Te distances in $Ni_9Te_6(PEt_3)_8$ are 2.86 and 2.54 Å, respectively, compared to the experimental values of 2.87 and 2.54 Å reported by Brennan et al.[18] In bare Ni_9Te_6, the distance between the central Ni to the rest of the 8 Ni atoms is ∼2.27 Å, which increases up to ∼2.50 Å in the presence of ligands. The binding with ligands reduced the bonding of the central Ni to the outer Ni sites. We would like to add that Nomikou et al. have shown how the atomic structure of Ni_9Te_6 can be obtained from a fragment of the bulk NiTe as ligands are attached to Ni sites.[32,33]

Since, the role of ligands is of critical importance, it is interesting to examine how strongly are the ligands bound to the cluster? Do the ligands merely protect the cluster or do they play a more active role in formulating an electron donor building block? Therefore, we calculated the atomization energy (AE) of the free cluster and the binding energy (BE) per ligand for the ligated species. The AE of Ni_9Te_6 was calculated using eq 1:

$$\mathrm{AE} = 9E(\mathrm{Ni}) + 6E(\mathrm{Te}) - E(\mathrm{Ni_9Te_6}) \quad (1)$$

where E(Ni), E(Te), and $E(Ni_9Te_6)$ are the total energies of a Ni and Te atom and a Ni_9Te_6 cluster, respectively. The AE/atom, an indication of the bonding in the metallic core is found to be 3.66 eV/atom. This energy is typical of bond strength in chalcogenide systems. To examine how strongly are the ligands bound to the core cluster, we calculated the BE per ligand via the eq 2:

$$\mathrm{BE} = [E(\mathrm{Ni_9Te_6}) + 8E(\mathrm{PEt_3}) - E(\mathrm{Ni_9Te_6(PEt_3)_8}]/8 \quad (2)$$

where $E(PEt_3)$ and $E(Ni_9Te_6(PEt_3)_8)$ are the total energies of PEt_3 and $Ni_9Te_6(PEt_3)_8$, respectively. Our studies indicate a BE

DOI: 10.1021/jacs.5b10986
J. Am. Chem. Soc. 2016, 138, 1916−1921

of 1.23 eV, showing that the ligands are not strongly bound to the clusters. The low binding energy of ligands is consistent with experimental observation that these ligands can readily dissociate in solution to form larger cluster.[34] Yet, the ligands have an appreciable effect on the electronic properties of the cluster. In particular the addition of ligands seems to be crucial for promoting formation of the ionic phase. To investigate this role, we examined the vertical and adiabatic ionization potentials (VIP and AIP) through the energy differences between the neutral ground state and cationic cluster in the geometry of the neutral and in its ground-state geometry, respectively. The calculated values are collected in Table 1. The

Table 1. VIP, AIP, the HOMO-LUMO Gap, and the Position of HOMO for Ni_9Te_6, $Ni_9Te_6(PH_3)_8$, and $Ni_9Te_6(PEt_3)_8$ Clusters

clusters	AIP (eV)	VIP (eV)	HL gap (eV)	HOMO (eV)
Ni_9Te_6	5.87	5.88	0.34	−4.06
$Ni_9Te_6(PH3)_8$	4.64	4.68	0.32	−3.17
$Ni_9Te_6(PEt_3)_8$	3.36	3.39	0.35	−2.08

VIP of bare Ni_9Te_6 is 5.88 eV, much higher than the alkali atoms. However, the addition of ligands reduces the VIP to 3.39 eV and AIP to 3.36 eV, which are less than those for a Cs atom and illustrates the importance of ligands in promoting a superalkali character. The low IP is required for the formation of ionic solid, as the EA of a C_{60} is around 2.68 eV.[35] In fact, the reduction in VIP with the addition of ligands to Ni_9Te_6 turns out to be more general. When PEt_3 ligands were replaced by phosphine (PH_3), the VIP of $Ni_9Te_6(PH_3)_8$ was found to be 4.68 eV, lower than that of Ni_9Te_6. Note that AIP's of the clusters are very close to corresponding VIP's. This can be understood from the fact that ground-state structures of cationic clusters are similar to those of neutrals.

The substantial decrease in VIP (by 2.49 eV) as the ligands are attached is fairly surprising particularly since the ligands are bound only by 1.23 eV to the metallic core. Also, the VIP of PEt_3 ligand is 7.98 eV, much higher than that of Ni_9Te_6. To examine this intriguing phenomenon, we first show in Figure 2 the one-electron energy levels of the bare Ni_9Te_6, $Ni_9Te_6(PH_3)_8$, and $Ni_9Te_6(PEt_3)_8$ clusters. Because of symmetric structures, a number of electron energy levels are found to be bunched near the HOMO−LUMO gap. The values of HOMO−LUMO gaps are tabulated in Table 1. A close inspection of the electronic energy spectrum reveals that the entire spectrum of Ni_9Te_6 is pushed up toward higher energies upon ligation. For example, the positions of HOMO in the majority spin channel of Ni_9Te_6, $Ni_9Te_6(PH_3)_8$, and $Ni_9Te_6(PEt_3)_8$ are found to be −4.06, −3.17, and −2.08 eV, respectively. Therefore, the HOMO's in $Ni_9Te_6(PH_3)_8$ and $Ni_9Te_6(PEt_3)_8$ shift up in energy by 0.99 and 1.98 eV compared to Ni_9Te_6. While the role of ligands in protecting the clusters is well-known, here ligands facilitate the formation of the ionic compound by altering the electronic structure of the cluster.

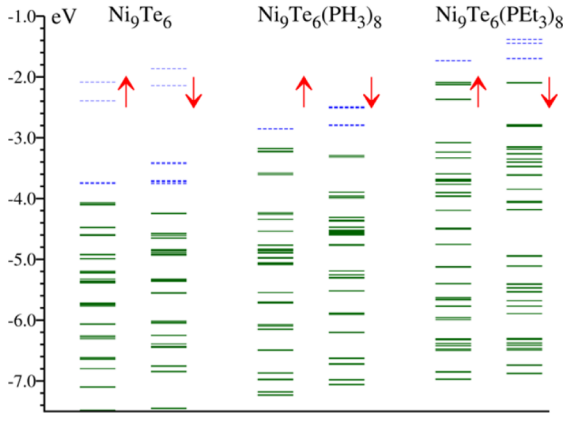

Figure 2. One-electron energy levels in the Ni_9Te_6, $Ni_9Te_6(PH_3)_8$, and $Ni_9Te_6(PEt_3)_8$ clusters. The up and down arrows denote the energy levels for the majority and minority spin channels, respectively. The filled and empty levels are represented by solid and dashed lines, respectively.

To uncover the microscopic mechanism, the local charge on the atoms of bare and ligated clusters was examined using Bader's analysis.[36,37] The local charges are given in the Table SI-I. The average charges on a Ni and Te atom are found to be +0.11e and −0.17e, respectively, in Ni_9Te_6. On the other hand, Te atoms have a slightly more negative charge (∼ −0.22e/atom), and Ni atoms are less positively charged (∼ +0.045e/atom) in the presence of PEt_3 ligands. Therefore, in addition to covalent bonding, the ligands can be thought of creating a crystal field due to excess negative charge. Also, each P site has a positive charge of +1.14e.

In order to examine the effect of crystal field on the electronic structure, single point calculations were performed on a Ni_9Te_6 surrounded by negative fictitious point charge as implemented in ADF. To find out the appropriate magnitude of point charges, we first carried out a Hirshfeld charge analysis[38] for Ni_9Te_6 and $Ni_9Te_6(PH_3)_8$, which are shown in Table SI-II (the memory limitations did not allow us to study $Ni_9Te_6(PEt_3)_8$ in the ADF code). Evidently, an excess of negative charge of −0.37e is present at Ni_9Te_6 upon ligation with PH_3 ligands. Since Te sites are all negatively charged, an average value of −0.061e is assigned to six fictitious charges situated at 0.50 Å from Te atoms. Figure 3 shows the partial density of states (PDOS) of isolated Ni_9Te_6, with point charges, and $Ni_9Te_6(PH_3)_8$. The HOMO of Ni_9Te_6 in Figure 3b relative to bare Ni_9Te_6 is shifted to higher energy. More specifically, not only the positions of HOMO's in Figure 3b,c are at the similar energies but also the peaks in DOS are shifted. Thus, the presence of ligands induces an internal electrostatic coulomb potential well by charging the Ni_9Te_6 that lifts its quantum states. As a result, the VIP of ligated species is found to be 1.14 eV lower than that of bare Ni_9Te_6. The one-electron energy levels and AIP's of Ni_9Te_6 and $Ni_9Te_6(PH_3)_8$ based on ADF are given in Table SI-III and Figure SI-I, respectively. Note also that the states near the Fermi energy are predominantly 3d-Ni states for both $Ni_9Te_6(PH_3)_8$ and $Ni_9Te_6(PEt_3)_8$ (Figure SI-II), indicating that the charge is transferred from 3d-states to unoccupied states of C_{60} during the formation of the ionic solid. To check, we performed the Bader charge analysis for optimized $Ni_9Te_6(PEt_3)_8C_{60}$ functional unit that shows −0.64e charge on C_{60}, which is consistent with above results. These calculations confirm that the role of ligands in controlling VIP as deduced above is general. Consequently, the ligands help stabilize the cluster solid.

We now examine the effect of ligands on the magnetic properties. The Ni_9Te_6 has a magnetic moment of 6 μ_B, where the Ni sites contribute a spin magnetic moment of 4.56 μ_B, while the Te contributes 0.516 μ_B. These contributions change slightly as the cluster is ligated with PEt_3, where the total local spin magnetic moment of $Ni_9Te_6(PEt_3)_8$ core is 5.33 μ_B, which

DOI: 10.1021/jacs.5b10986
J. Am. Chem. Soc. 2016, 138, 1916−1921

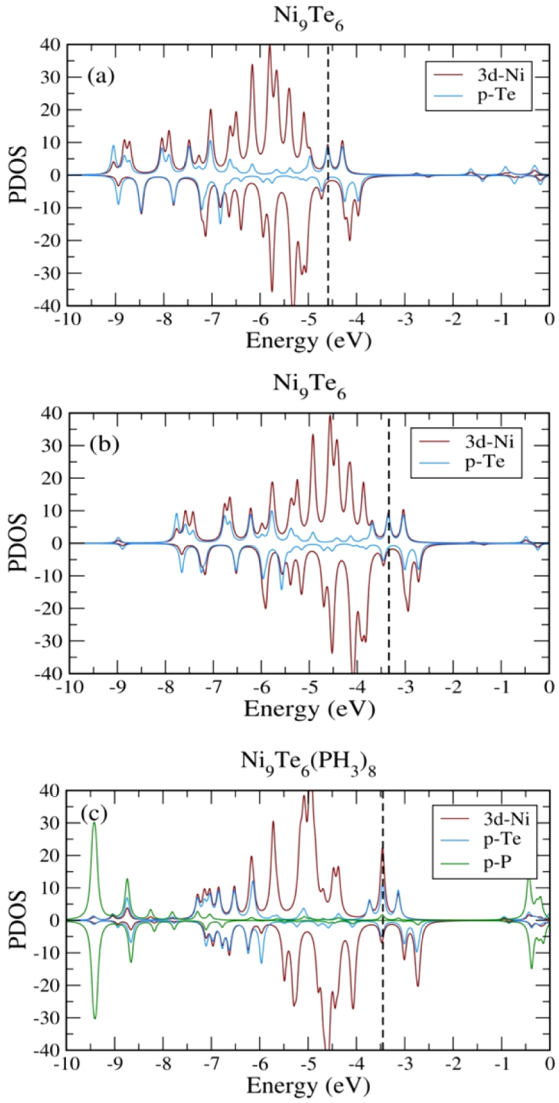

Figure 3. PDOS of the 3d Ni and p Te states for (a) bare Ni_9Te_6 and (b) Ni_9Te_6 in the presence of six fictitious point charges. (c) The PDOS between the 3d-Ni, p-Te, and p-P states for $Ni_9Te_6(PH_3)_8$. The Fermi energy levels are shown by dashed vertical energy lines in black color.

is close to the estimated value of 5.4 μ_B based on the SQUID measurements. The contributions to total magnetic moment from Ni and Te sites are found to be 4.49 and 0.69 μ_B, respectively. The P atoms of ligands also carry a small moment of 0.10 μ_B. To examine how strongly the moments are coupled to each other, we calculated the energy difference between the ground state and an excited state where one of the spins was flipped. The energy difference between the states with spin of 6 μ_B and 4 μ_B was found to be 0.21 eV that corresponds to a temperature of 2436 K. The strong exchange coupling determines the dynamical behavior of the magnetic moment of $Ni_9Te_6(PEt_3)_8$ that we now consider.

It is now fairly well-known that a nanomagnet with size smaller than the typical domain size has exchange coupled atomic moments. Such a particle behaves like a giant magnet with a moment $N\mu$, where N is the number of atoms, while μ is the moment per atom.[39−42] The reduction in size, however, reduces the MAE responsible for keeping the magnetization oriented in certain directions and becomes comparable to the thermal energy.[42] At temperatures above the blocking temperature, the clusters can then undergo superparamagnetic relaxations where the giant moment undergoes fluctuations in direction. To examine if the $Ni_9Te_6(PEt_3)_8$ clusters undergo these relaxations, we proceeded to calculate the MAE. It is well-known that MAE in small atomic clusters is largely due to magneto-crystalline anisotropy arising due to spin−orbit coupling.[43]

To calculate the MAE, we calculated the change in energy of the system as the magnetization was oriented along different directions. The MAE is the difference in energy along the easy axis (minimum energy) and the hard axis (maximum energy). The MAE landscape showing the variation of the energy for various values of θ and ϕ is shown in Figure 4. Within a Néel

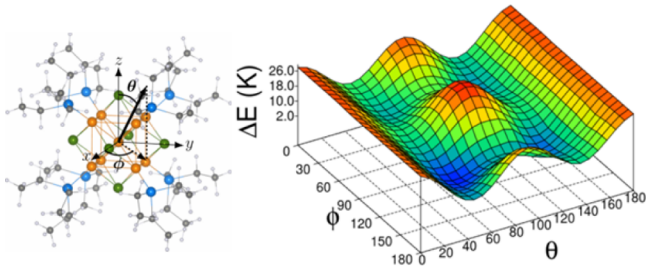

Figure 4. Energy landscape for the magnetization direction as a function of ϕ and θ.

model[44] with an attempt frequency of a GHz, this corresponds to relaxation time of around 10^{-8} s at a temperature of 10 K. This shows that the observed paramagnetic behavior around 10 K really correspond to superparamagnetic relaxations. Further, the easy axis lie along [111], i.e., body diagonal Ni−Ni directions, while the hard axis are along the [100] directions, i.e., Ni−Te bonds as shown in Figure 1. The values of orbital angular moment along easy and hard axes, i.e., L_{easy} and L_{hard} are found to be 0.194 and 0.205 μ_B, respectively. The small value of MAE can also be related to minor variation in the orbital angular momentum.

The material also exhibits a phase transition below 4 K as seen through the change in magnetization if the sample is cooled in zero field or in a large field. Further, the material exhibits a hysteresis loop in the measurements around 2 K. Previous studies on C_{60} complexes including C_{60}-tetrakis ethylene have also shown hysteresis loops at very low temperatures, but the coercive fields (1.6 G) are very low.[45] The corresponding coercive fields in $Ni_9Te_6(PEt_3)_8$ are around 400 Oe, indicating that the hysteresis is not due to C_{60} alone. The ferromagnetic state below 4 K, therefore, suggests a cooperative phenomenon where the ligated Ni_9Te_6 clusters interact via the C_{60} molecules. To explore if the C_{60} could mediate a weak indirect exchange interaction, we examined an assembly of two $Ni_9Te_6(PH_3)_8$ clusters separated by a C_{60} as shown in Figure SI-IV. We took $Ni_9Te_6(PH_3)_8$ rather than $Ni_9Te_6(PEt_3)_8$ to keep the calculations manageable. In particular, we examined the change in energy as the spin moments on the two $Ni_9Te_6(PH_3)_8$ clusters were aligned parallel and antiparallel to each other. The calculations predict a ferromagnetic ground state, while the antiferromagnetic state was only 7.7 meV higher in energy. These results indicate a weak superexchange interaction between the clusters mediated by C_{60}. For the larger $Ni_9Te_6(PEt_3)_8$ clusters, the difference is expected to be smaller. Nevertheless, we believe that a similar

DOI: 10.1021/jacs.5b10986
J. Am. Chem. Soc. 2016, 138, 1916−1921

superexchange in $Ni_9Te_6(PEt_3)_8C_{60}$ stabilizes the ferromagnetic state at low temperature. While the origin of the superexchange interaction is not established, one possibility may be to invoke a intra-C_{60} Jahn−Teller (J-T) distortion due to partial charge transfer similar to that proposed by Kawamoto to account for weak ferromagnetism in C_{60}-TDAE system.[46] A bare C_{60} is marked by three unoccupied orbitals. The bonding of spin up orbitals in two $Ni_9Te_6(PEt_3)_8$ clusters and one of the three unoccupied orbitals in C_{60} would lead to a bonding state consistent with our calculations that indicate a partial charge transfer to C_{60}. As there are three unfilled states in C_{60}, the occupation of one state would result in J-T distortion (structural) to stabilize the bonding state, as a structural distortion lowers the energy of one orbital while it raises the energy of others.[46] Such distortion could stabilize the ferromagnetic state. Our calculations show that the MAE is sensitive to the charge state of the cluster. For example, the MAE for a cationic $Ni_9Te_6(PEt_3)_8$ is 107.83 K as opposed to 31.55 K for the neutral $Ni_9Te_6(PEt_3)_8$. The MAE landscape of cationic $Ni_9Te_6(PEt_3)_8$ is given in Figure SI-III. As pointed out in our earlier papers, the anisotropy tensor involves matrix elements between occupied and unoccupied states and hence is sensitive to the separation between occupied and unoccupied manifolds.[47] Since the electronic structure is sensitive to the charged state, the MAE can change with the charge. We also find that the direction of the easy axis changes upon charging. Since the charge on superatoms depends on the separation and the size, these findings may help understand the experiments on[33] $Ni_9Te_6(PMe_3)_8C_{60}$ and on $Ni_9Te_6(PEt_3)_8C_{70}$ that exhibit a different T_M.

CONCLUSIONS

The present work shows that the newly synthesized $Ni_9Te_6(PEt_3)_8C_{60}$ chalcogenide superatomic solid is composed of superalkali $Ni_9Te_6(PEt_3)_8$ clusters that donate charge to C_{60} to stabilize the ionic solid. The formation of the solid is promoted by ligands that reduce the ionization potential of the ligated clusters through a charge transfer. This phenomena is not specific to PEt_3 ligands, as shown in the case of ligation with phosphine. $Ni_9Te_6(PEt_3)_8$ is also shown to be marked by a large intracluster exchange and a weak MAE. The combination leads to superparamagnetic relaxations above 4 K, where each cluster behaves as a giant magnet whose orientation undergoes fluctuations in direction. The solid is also marked by a weak superexchange coupling mediated via C_{60} that leads to a ferromagnetic ordering at very low temperatures. The MAE is sensitive to the charged state of the cluster and can be modulated by changing the charged state of the cluster through changing ligands or larger anions. To summarize, $Ni_9Te_6(PEt_3)_8C_{60}$ can be regarded as superalkali, superparamagnetic superatomic solid.

ASSOCIATED CONTENT

Supporting Information

The Supporting Information is available free of charge on the ACS Publications website at DOI: 10.1021/jacs.5b10986.

Supporting Information includes Bader (VASP)/Hirshfeld (ADF) charges, one electron energy levels (ADF) and PDOS (VASP), optimized Cartesian coordinates, and total energies of bare and ligated Ni_9Te_6 clusters. Ground-state structure and MAE landscape of $Ni_9Te_6(PEt_3)_8^+$ are also provided (PDF)

AUTHOR INFORMATION

Corresponding Author

*snkhanna@vcu.edu

Notes

The authors declare no competing financial interest.

ACKNOWLEDGMENTS

We gratefully acknowledge funding support from the Department of Energy under award no. DE-SC0006420. Part of the computations used the resources of the National Energy Research Scientific Computing Center (NERSC) and cluster computing facility in the HRI (http://www.hri.res.in/cluster) Allahabad. We thank DOE office of Science User Facility supported by the Office of the U.S. Department of Energy under contract no. DE-C0205CH11231.

REFERENCES

(1) Khanna, S. N.; Jena, P. *Phys. Rev. B: Condens. Matter Mater. Phys.* **1995**, *51* (19), 13705.
(2) Castleman, A. W.; Khanna, S. N. *J. Phys. Chem. C* **2009**, *113* (7), 2664.
(3) Claridge, S. A.; Castleman, A. W.; Khanna, S. N.; Murray, C. B.; Sen, A.; Weiss, P. S. *ACS Nano* **2009**, *3* (2), 244.
(4) Mandal, S.; Reber, A. C.; Qian, M.; Weiss, P. S.; Khanna, S. N.; Sen, A. *Acc. Chem. Res.* **2013**, *46*, 2385.
(5) Nakaya, M.; Iwasa, T.; Tsunoyama, H.; Eguchi, T.; Nakajima, A. *Nanoscale* **2014**, *6* (24), 14702.
(6) Jadzinsky, P. D.; Calero, G.; Ackerson, C. J.; Bushnell, D. A.; Kornberg, R. D. *Science* **2007**, *318* (5849), 430.
(7) Turkiewicz, A.; Paley, D. W.; Besara, T.; Elbaz, G.; Pinkard, A.; Siegrist, T.; Roy, X. *J. Am. Chem. Soc.* **2014**, *136* (45), 15873.
(8) Neukermans, S.; Janssens, E.; Chen, Z. F.; Silverans, R. E.; Schleyer, P. v. R.; Lievens, P. *Phys. Rev. Lett.* **2004**, *92* (16), 163401.
(9) Goicoechea, J. M.; McGrady, J. E. *Dalton Trans* **2015**, *44* (15), 6755.
(10) Bergeron, D. E.; Roach, P. J.; Castleman, A. W.; Jones, N. O.; Khanna, S. N. *Science* **2005**, *307* (5707), 231.
(11) Reveles, J. U.; Clayborne, P. A.; Reber, A. C.; Khanna, S. N.; Pradhan, K.; Sen, P.; Pederson, M. R. *Nat. Chem.* **2009**, *1* (4), 310.
(12) Kumara, C.; Aikens, C. M.; Dass, A. *J. Phys. Chem. Lett.* **2014**, *5* (3), 461.
(13) Clayborne, P. A.; Lopez-Acevedo, O.; Whetten, R. L.; Grönbeck, H.; Häkkinen, H. *J. Chem. Phys.* **2011**, *135* (9), 094701.
(14) Zeng, C.; Liu, C.; Chen, Y.; Rosi, N. L.; Jin, R. *J. Am. Chem. Soc.* **2014**, *136* (34), 11922.
(15) Jian, N.; Palmer, R. E. *J. Phys. Chem. C* **2015**, *119* (20), 11114.
(16) Negishi, Y.; Iwai, T.; Ide, M. *Chem. Commun.* **2010**, *46* (26), 4713.
(17) Roy, X.; Lee, C.-H.; Crowther, A. C.; Schenck, C. L.; Besara, T.; Lalancette, R. A.; Siegrist, T.; Stephens, P. W.; Brus, L. E.; Kim, P.; Steigerwald, M. L.; Nuckolls, C. *Science* **2013**, *341* (6142), 157.
(18) Brennan, J. G.; Siegrist, T.; Stuczynski, S. M.; Steigerwald, M. L. *J. Am. Chem. Soc.* **1989**, *111* (26), 9240.
(19) Lee, C.-H.; Liu, L.; Bejger, C.; Turkiewicz, A.; Goko, T.; Arguello, C. J.; Frandsen, B. A.; Cheung, S. C.; Medina, T.; Munsie, T. J. S.; D'Ortenzio, R.; Luke, G. M.; Besara, T.; Lalancette, R. A.; Siegrist, T.; Stephens, P. W.; Crowther, A. C.; Brus, L. E.; Matsuo, Y.; Nakamura, E.; Uemura, Y. J.; Kim, P.; Nuckolls, C.; Steigerwald, M. L.; Roy, X. *J. Am. Chem. Soc.* **2014**, *136* (48), 16926.
(20) Perdew, J. P.; Yue, W. *Phys. Rev. B: Condens. Matter Mater. Phys.* **1986**, *33* (12), 8800.
(21) Blöchl, P. E. *Phys. Rev. B: Condens. Matter Mater. Phys.* **1994**, *50* (24), 17953.
(22) Payne, M. C.; Teter, M. P.; Allan, D. C.; Arias, T. A.; Joannopoulos, J. D. *Rev. Mod. Phys.* **1992**, *64* (4), 1045.
(23) Teter, M. P.; Payne, M. C.; Allan, D. C. *Phys. Rev. B: Condens. Matter Mater. Phys.* **1989**, *40* (18), 12255.

DOI: 10.1021/jacs.5b10986
J. Am. Chem. Soc. 2016, 138, 1916−1921

(24) *VASP* http://cms.mpi.univie.ac.at/vasp/vasp/vasp.html (accessed Sep 14, 2015).
(25) Van Lenthe, E.; Baerends, E. J. *J. Comput. Chem.* **2003**, *24* (9), 1142.
(26) van Lenthe, E.; Baerends, E. J.; Snijders, J. G. *J. Chem. Phys.* **1993**, *99* (6), 4597.
(27) van Lenthe, E.; Ehlers, A.; Baerends, E.-J. *J. Chem. Phys.* **1999**, *110* (18), 8943.
(28) Kresse, G.; Hafner, J. *Phys. Rev. B: Condens. Matter Mater. Phys.* **1993**, *47* (1), 558.
(29) Kresse, G.; Furthmüller, J. *Phys. Rev. B: Condens. Matter Mater. Phys.* **1996**, *54* (16), 11169.
(30) Guerra, C. F.; Snijders, J. G.; Te Velde, G.; Baerends, E. J. *Theor. Chem. Acc.* **1998**, *99* (6), 391.
(31) te Velde, G.; Bickelhaupt, F. M.; Baerends, E. J.; Fonseca Guerra, C.; van Gisbergen, S. J. A.; Snijders, J. G.; Ziegler, T. *J. Comput. Chem.* **2001**, *22* (9), 931.
(32) Wheeler, R. A. *J. Am. Chem. Soc.* **1990**, *112* (24), 8737.
(33) Nomikou, Z.; Schubert, B.; Hoffmann, R.; Steigerwald, M. L. *Inorg. Chem.* **1992**, *31* (11), 2201.
(34) Steigerwald, M. L.; Stuczynski, S. M.; Kwon, Y.-U.; Vennos, D. A.; Brennan, J. G. *Inorg. Chim. Acta* **1993**, *212* (1), 219.
(35) Wang, X.-B.; Ding, C.-F.; Wang, L.-S. *J. Chem. Phys.* **1999**, *110* (17), 8217.
(36) Bader, R. F. W. *Atoms in Molecules: A Quantum Theory (The International Series of Monographs on Chemistry)*; Oxford University Press: New York, 1990.
(37) Henkelman, G.; Arnaldsson, A.; Jónsson, H. *Comput. Mater. Sci.* **2006**, *36* (3), 354.
(38) Hirshfeld, F. L. *Theor. Chim. Acta* **1977**, *44* (2), 129.
(39) Khanna, S. N.; Linderoth, S. *Phys. Rev. Lett.* **1991**, *67* (6), 742.
(40) Mannini, M.; Pineider, F.; Sainctavit, P.; Danieli, C.; Otero, E.; Sciancalepore, C.; Talarico, A. M.; Arrio, M.-A.; Cornia, A.; Gatteschi, D.; Sessoli, R. *Nat. Mater.* **2009**, *8* (3), 194.
(41) Khajetoorians, A. A.; Wiebe, J. *Science* **2014**, *344* (6187), 976.
(42) El-Gendy, A. A.; Qian, M.; Huba, Z. J.; Khanna, S. N.; Carpenter, E. E. *Appl. Phys. Lett.* **2014**, *104* (2), 023111.
(43) Błoński, P.; Hafner, J. *Phys. Rev. B: Condens. Matter Mater. Phys.* **2009**, *79* (22), 224418.
(44) Bean, C. P.; Livingston, J. D. *J. Appl. Phys.* **1959**, *30* (4), S120.
(45) Suzuki, A.; Suzuki, T.; Whitehead, R. J.; Maruyama, Y. *Chem. Phys. Lett.* **1994**, *223* (5−6), 517.
(46) Kawamoto, T. *Solid State Commun.* **1997**, *101* (4), 231.
(47) Pederson, M. R.; Khanna, S. N. *Phys. Rev. B: Condens. Matter Mater. Phys.* **1999**, *60* (13), 9566.

DOI: 10.1021/jacs.5b10986
J. Am. Chem. Soc. 2016, 138, 1916−1921